# High Performance Star Block Aliphatic Polyester Thermoplastic Elastomers using PDLA-b-PLLA Stereoblock Hard Domains

Stephanie Liffland,† Margaret Kumler,† and Marc. A. Hillmyer†\*

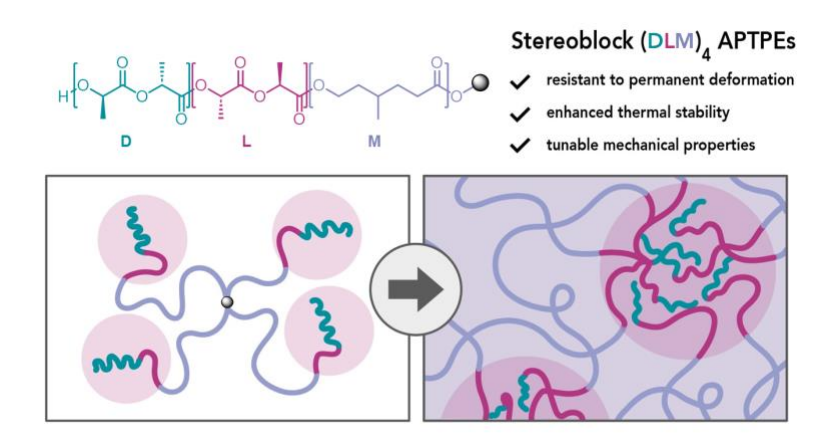
<sup>†</sup>Department of Chemistry, University of Minnesota, Minnesota, Minnesota 55455-0431, United States of America

\*To whom correspondence should be addressed:

Email: hillmyer@umn.edu

Submitted as a Letter to ACS Macro Letters

## TOC graphic



#### Abstract

Star block (ABC)<sub>4</sub> terpolymers consisting of a rubbery poly(γ-methyl-ε-caprolactone) (PγMCL) (C) core and hard poly(L-lactide) (PLLA) (B) and poly(D-lactide) (PDLA) (A) end-blocks with varying PDLA to PLLA block ratios were explored as high-performance, sustainable, aliphatic polyester thermoplastic elastomers (APTPEs). The stereocomplexation of the PDLA/PLLA blocks within the hard domains provided the APTPEs with enhanced thermal stability and an increased resistance to permanent deformation compared to non-stereocomplex analogues. Variations in the PDLA:PLLA block ratio yielded tunable mechanical properties likely due to differences in the extent and location of stereocomplex crystallite formation as a result of architectural constraints. This work highlights the improvements in mechanical performance due to stereocomplexation within the hard domains of these APTPEs and the tunable nature of the hard domains to significantly impact material properties, furthering the development of sustainable materials that are competitive with current industry standard materials.

Thermoplastic elastomers (TPEs) have wide ranging applications in adhesives, personal care products, automotive parts, and many other commercial goods due to their tunable properties and processability unlike traditionally chemically crosslinked elastomers. The archetypal example of a TPE is an ABA triblock polymer with hard (high- $T_g$  or  $-T_m$ ) A blocks as the minority component covalently connected to a soft (low- $T_g$ ) midblock (B). Block incompatibility-driven microphase separation typically produces A domains embedded in a matrix of B, resulting in a physically crosslinked network. Trapped entanglements within the rubbery B midblocks, in combination with the physical crosslinks through the hard domains, result in characteristically high tensile strength, toughness, and elastic recovery properties. Styrenic TPEs, containing hard polystyrene (PS) end-blocks and polydiene midblocks, comprise the majority of commercial materials due to their relatively low cost and versatility. However, there is a large disparity between usage and material lifetimes, the latter of which can be centuries in a landfill, for these petroleum-based and essentially non-degradable polymers.

Sustainable alternatives to incumbent petrochemical-derived TPEs that display competitive mechanical properties but are more readily degraded at their end-of-life are being actively pursued.<sup>5–13</sup> For example, aliphatic polyesters TPEs (APTPEs) can be prepared from biomass and are susceptible to hydrolytic degradation that facilitates biodegradation under conducive conditions. Polylactide (PLA), which is both low cost and commercially available, has been widely utilized for the hard domains of APTPEs as its thermal and mechanical properties are comparable to PS.<sup>14</sup> Previous ABA-type APTPEs comprised of semicrystalline poly(L-lactide) (PLLA) as the hard domains and poly(γ-methyl-ε-caprolactone) (PγMCL) as the soft blocks have exhibited impressive mechanical properties with ultimate tensile strengths (σ<sub>B</sub>), elongations at break (ε<sub>B</sub>), and resiliencies comparable with commercial styrenic materials.<sup>10</sup>

Star block APTPE architecture further improves mechanical performance due in part to the ability for the core block domains to more effectively distribute applied stresses throughout the network.<sup>12</sup> The star architecture also helps to mitigate the impact of stress relaxation, which can result in undesirable creep behavior. The star APTPEs (PLLA-*b*-PγMCL)<sub>n</sub> ((LM)<sub>n</sub>) have impressive mechanical properties; however, semicrystalline PLLA displays considerably slower crystallization rates than other commercially useful semicrystalline thermoplastic materials.<sup>15,16</sup> This sluggish crystallization of PLLA is undesirable for commercially-relevant processing methods such as injection molding; thus improvements are needed.

Polylactide can be synthesized using racemic D,L-lactide to provide amorphous, atactic PLA, or using L-lactide (or D-lactide) to yield semicrystalline, isotactic PLLA (or PDLA).  $^{17,18}$  Blending of PLLA and PDLA results in co-crystallized PDLA/PLLA stereocomplex crystallites (SCs) that are distinct from homopolymer crystallites (HCs).  $^{19,20}$  SCs exhibit a melting temperature significantly higher than that of HCs ( $T_{m,SC} \approx 230$  °C;  $T_{m,HC} \approx 180$  °C) and have improved resistance to hydrolysis,  $^{21}$  increased tensile moduli,  $^{22}$  more rapid crystallization kinetics,  $^{23,24}$  and enhanced thermal stability.  $^{25}$  The improved properties are thought to arise from stabilization of the stereocomplex crystal structure, which consists of 31-helices of opposite configuration, with strong van der Waals interactions that allow for specific energetic interaction-driven packing.  $^{26,27}$ 

In addition to PDLA/PLLA blends, there have been many reports on the synthesis and properties of PDLA/PLLA stereoblock polymers of varying architectures.<sup>28–38</sup> The stereoblock architecture has been shown to provide more facile stereocomplex crystallization than in analogous 1:1 PDLA:PLLA blends due to the close proximity of the neighboring enantiomeric PDLA and PLLA blocks. There have been reports of both star PLLA-*b*-PDLA stereo diblock polymers<sup>35–37</sup> and linear ABCBA stereo pentablock copolymers.<sup>39–41</sup>

Here we report the synthesis of 4-arm stereoblock star terpolymers (PDLA–PLLA–P $\gamma$ MCL)4 ((DLM)4) to yield high performance APTPEs. We posit that PDLA/PLLA stereocomplexation within the hard domains will provide enhanced thermal stability and will mitigate undesirable stress relaxation and further improve tensile properties in these materials. A set of 4-arm star block APTPEs with a constant overall volume fraction of polylactide but differing PDLA to PLLA (D:L) block ratios were prepared and studied. D:L block ratios of 1:2, 1:1, 2:1, and 3:1 at a fixed volume fraction of polylactide ( $f_{LA} \cong 0.30$ ) were targeted to probe the effect of symmetric and asymmetric stereoblock hard domains on material performance as compared to a star APTPE with PLLA-only end-blocks (0:1).

We first synthesized tetrafunctional (PγMCL)<sub>4</sub> star polymers by Sn(Oct)<sub>2</sub>-catalyzed ring opening transesterification polymerization (ROTEP) of γMCL in the melt (**Figure 1**).<sup>10</sup> The hydroxy-telechelic (PγMCL)<sub>4</sub> core was then used as a macroinitiator for the ROTEP of L-lactide. Sn(Oct)<sub>2</sub> was used due to the need for a high degree of stereoretention in the PLLA and PDLA blocks.<sup>12,18,42</sup> Successful star synthesis was indicated by disappearance of the end-group resonances for the (PγMCL)<sub>4</sub> core and appearance of resonances that correspond to the PLLA end groups by <sup>1</sup>H NMR spectroscopy (**Figure S1**). In the third step, the Sn(Oct)<sub>2</sub>-catalyzed ROTEP of D-lactide was performed using the (LM)<sub>4</sub> stars as a tetrafunctional macroinitiator. Formation of the (DLM)<sub>4</sub> stereoblock star polymers was evidenced by <sup>1</sup>H NMR spectroscopy through comparative integration of the polylactide resonances (**Figure S2**) and by size exclusion chromatography (SEC) traces (**Figure S3**) from the shift toward lower elution times in the stereoblock compared to the parent (LM)<sub>4</sub> (**Table S1**). The 5 samples studied here are labeled

according to the stereochemistry of the polylactide blocks (DLM or LM) followed by the D:L block mass ratio (e.g., DLM-1:1).

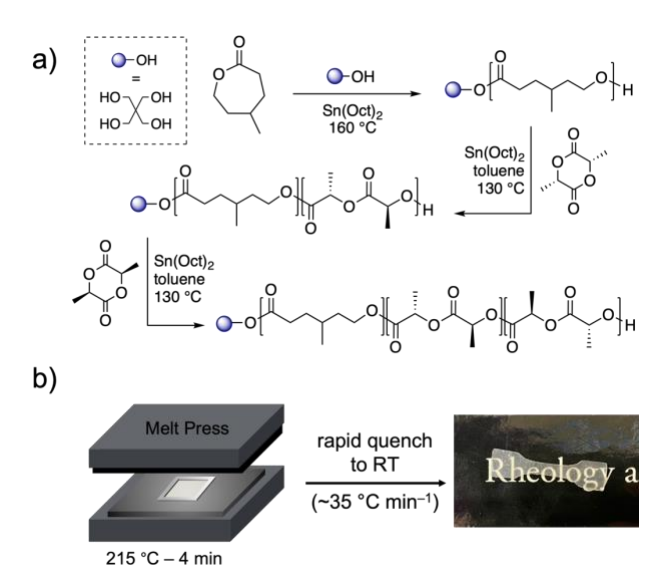


**Figure 1.** a) Representative synthesis of DLM 4-arm star stereoblock terpolymers using pentaerythritol as the initiator and b) schematic detailing melt processing conditions employed for processing.

We processed the samples at a temperature below the order-disorder transition temperature (*T*<sub>ODT</sub>) to avoid undesirable crystallization-induced microphase separation from a homogenous melt. 11,43–45 Variable temperature small-angle X-ray scattering (SAXS) (**Figures S4-S8**) suggests that the *T*<sub>ODT</sub> for the samples is in the range of 230–240 °C (**Table S3**), therefore these materials were melt processed below 230 °C to promote crystallization from a microphase separated melt. Previous work has shown that SCs can act as heterogeneous nucleators for the crystallization of PLA HCs, which can impact the thermal and mechanical properties of the material. 16,23,24,28,29,46–51 Wide angle X-ray scattering (WAXS) patterns of all DLM stereoblocks (**Figures S13–S17**) display diffraction peaks characteristic of the stereocomplex after annealing at 220 °C for 10 min. For consistency, we used a processing temperature of 215 °C that provided an microphase

separated melt ( $T < T_{\rm ODT}$ ) in which SCs were present for all DLM samples (see Supporting Information). Processing at 215 °C also decreases the potential for degradation during processing given the observed degradation temperatures for related materials ( $T_{\rm d,5\%} \cong 245-260$  °C). <sup>10,11</sup> This processing protocol leverages the ability of SCs to promote further crystallization through nucleation, providing systems with decreased crystallization half times that are amenable to, for example, injection molding without the addition of nucleating agents. <sup>23</sup>

The modulus of the melt-pressed films under uniaxial extension was measured as a function of temperature by dynamic mechanical thermal analysis (DMTA) (Figure 2). The drops in storage modulus near -56 °C are due to the glass transition of PyMCL, corroborated by dynamic scanning calorimetry (DSC) measurements (Table 1). Interestingly, despite containing equivalent polylactide volume fractions and overall molar masses, the initial relatively invariant moduli values  $(E_{N,1})$  following the PYMCL glass transition for the APTPEs vary dramatically. The difference in material behavior is most clear in comparisons of the symmetric stereoblock, DLM-1:1 ( $E_{\rm N,1} = 1-10$  MPa), and the PLLA analogue, LM-0:1, ( $E_{\rm N,1} = 80-100$  MPa), which display the lowest and highest initial  $E_{\rm N,1}$  values, respectively. The remaining asymmetric stereoblocks fall in an intermediate range between these two extremes but exhibit a clear trend of increasing  $E_{\rm N,l}$ values with increasing PDLA block lengths (i.e.,  $E_{N,1}$  DLM-3:1 >  $E_{N,1}$  DLM-2:1 >  $E_{N,1}$  DLM-1:2). This variation in  $E_{N,1}$  is distinct from the behavior exhibited by (LM)<sub>n</sub> star APTPEs and for linear PLLA-b-PγMCL-b-PLLA triblock polymers, <sup>10,11</sup> which display similar initial moduli upon heating during DMTA experiments for samples with equivalent polylactide volume fractions ( $f_{LA}$ ). The difference between the  $E_{\rm N,1}$  values observed in the stereoblocks may be due to the proximity of stereocomplex to the domain interface (see below and Supporting Information).<sup>2,52</sup> However, the difference between the sample with the highest modulus, LM-0:1, and the remaining lower-moduli stereoblock samples may also be due to the formation of discrete and more-isometric, hard domains in samples with higher SC content, which could result in a filler effect that has a smaller consequence on the modulus of the material compared to more extended domains (e.g., cylinders).

**Table 1.** Thermal and mechanical properties of stereoblock star polymers.

Sample ID (Composi tion-D:L)	M <sub>n,tota</sub> l <sup>a</sup> (kDa)	$f_{\mathrm{LA}}_{b}$	M <sub>n,ar</sub> <sub>m,L</sub> (kDa )	$M_{ m n,ar}$ ${}_{ m m,D}{}^a$ (kDa	T <sub>m,HC</sub> d (°C)	T <sub>m,SC</sub> d (°C)	$\phi_c{}^e$	E <sup>f</sup> (MPa)	$\sigma_{ m B}^f$ (MPa)	ε <sub>B</sub> <sup>f</sup> (%)	Resid ual Strain	Recov ery <sup>h</sup> (%)	d <sup>i</sup> (n m)
LM-0:1	172	0.31	15.1	0	165		0.20	34.9 ± 2.6	41.2 ± 1.3	1150 ± 53	0.62- 0.70	77–79	35
DLM-1:2	162	0.30	9.0	4.9		210	0.39	$10.1 \pm 0.4$	43.8 ± 1.7	$1240 \\ \pm 97$	0.35- 0.43	86–88	33
DLM-1:1	158	0.29	6.0	6.8		211, 221	0.47	$12.3 \pm 0.8$	44.0 ± 4.2	1090 ± 63	0.42– 0.46	84–86	33
DLM-2:1	178	0.32	5.8	10.3		217	0.35	$20.7 \pm 0.7$	28.4 ± 1.6	930 ± 75	0.50– 0.51	83–84	36
DLM-3:1	181	0.33	4.4	12.3	126	207	0.29	$36.5 \pm 1.3$	$36.8 \pm 2.3$	1180 ± 69	0.65– 0.67	77–78	39

<sup>&</sup>lt;sup>a</sup> Estimated by <sup>1</sup>H NMR spectroscopy using end-group analysis. <sup>b</sup> Calculated using  $\rho_{PLLA} = 1.25$  g cm<sup>-3</sup> and  $\rho_{P\gamma MCL} = 1.037$  g cm<sup>-3</sup> at 25 °C. <sup>c</sup> First heat in DSC heating at 10 °C min<sup>-1</sup>. <sup>d</sup>Taken as the peak of melting endotherm on the first heating cycle at 10 °C min<sup>-1</sup> in DSC. <sup>e</sup> Crystalline fraction within PLA domains (φ<sub>c</sub>) calculated using the equation φ<sub>c</sub> =  $\Delta H_m/((w_{SC} \times \Delta H_{m,SC}))$ ), where  $\Delta H_{m,HC} = 93$  J g<sup>-1</sup>,  $\Delta H_{m,SC} = 142$  J g<sup>-1</sup>,  $\omega_{HC} = 142$  J g<sup>-1</sup>,  $\omega$ 

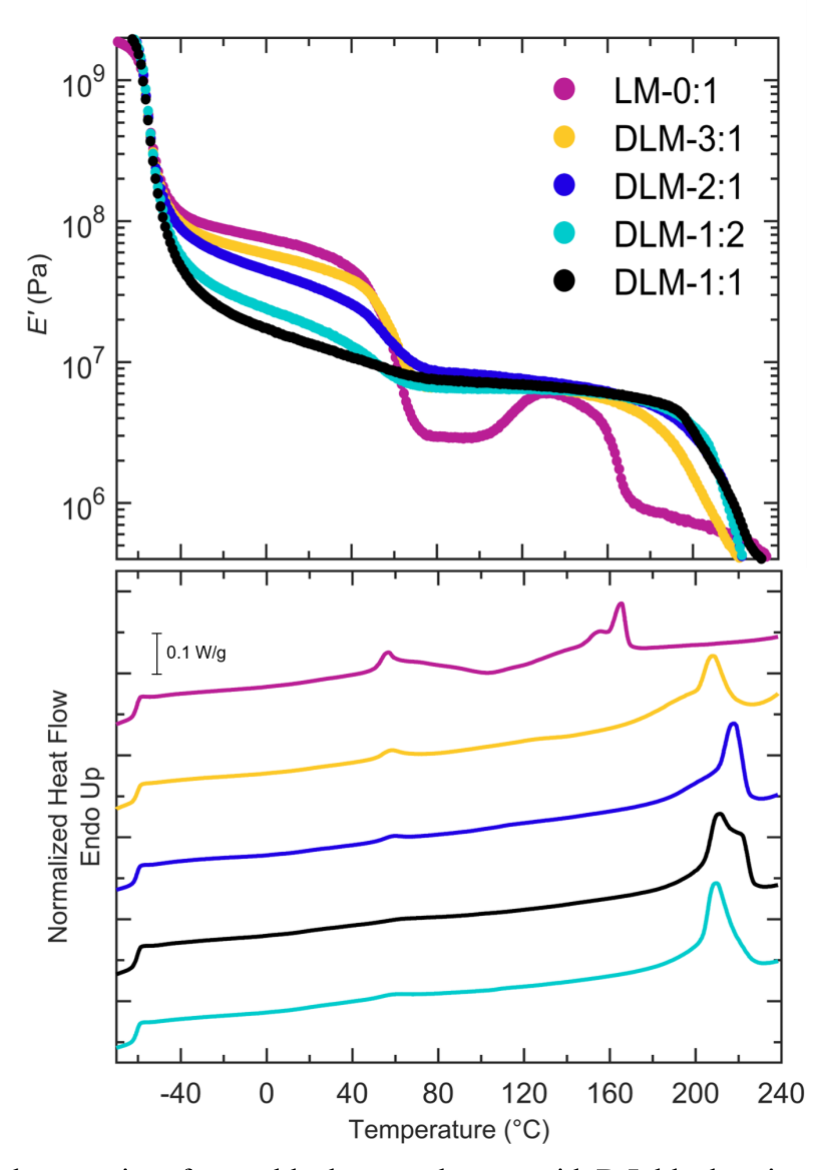


**Figure 2.** Thermal properties of stereoblock star polymers with D:L block ratios of 0:1 (magenta), 3:1 (yellow), 2:1 (blue), 1:1 (black), and 1:2 (aqua) analyzed by DMTA in tension upon heating as-processed samples at 5 °C min<sup>-1</sup> (top, 1 Hz, 0.05% strain) and DSC upon heating at 10 °C min<sup>-1</sup> (bottom, first heating cycle). DSC traces have been vertically shifted for clarity.

After passing through the PLA glass transition, the DLM stereoblocks all achieve the same plateau modulus ( $E_{\rm N,2}$  = 4–8 MPa) which can be attributed to trapped entanglements in the PγMCL blocks, which are expected to be consistent between samples as the molar masses of the PγMCL blocks are much greater than the entanglement molar mass,  $M_{\rm e}$  ( $M_{\rm n,PγMCL} \cong 120$  kg mol<sup>-1</sup>;  $M_{\rm e} \cong 2.9$ 

kg mol<sup>-1</sup>).<sup>10</sup> DLM-1:1, DLM-1:2, and DLM-2:1 maintain this plateau modulus until the onset of material softening at 200 °C due to melting of the SCs as confirmed by DSC (**Figure 2**). The softening temperature of DLM-3:1 is slightly lower than the other stereoblocks, with the modulus beginning to decrease gradually around 160 °C before precipitously dropping at ~190 °C. This behavior agrees with the low intensity melting endotherm at 157 °C by DSC for DLM-3:1, indicating the presence of HCs in the sample. The LM-0:1 analogue exhibited a much lower plateau modulus than the DLM samples following the polylactide  $T_g$ . We observed recovery of the modulus due to cold crystallization of PLLA from ~110–130 °C, which was corroborated by the exothermic signal in DSC over this temperature interval.

The high melting temperature of the SCs results in significantly elevated softening temperatures for the DLM stereoblocks compared to the LM analogue. The high thermal stability provides a remarkably wide usable temperature range for these APTPEs. Additionally, the observed spread in the modulus at  $T_{g,P\gamma MCL} < T < T_{g,PLA}$  (i.e., the typical usage window) for the DLM stereoblocks suggests that a range of mechanical characteristics can be achieved for systems with equivalent volume fractions of PLA, simply by changing the D:L ratios.

Room temperature SAXS patterns for the DLM stereoblocks can be seen in **Figure 3**. All DLM stereoblocks display a broad principal scattering peak,  $q^*$ , at 0.16–0.19 nm<sup>-1</sup> ( $d = 2\pi/q^* = 33-39$  nm), with no higher-order reflections. These domain spacings are comparable to TPEs with similar compositions and molar masses. <sup>6,10,12,57</sup> While all of these samples are microphase separated, the absence of distinct higher-order peaks indicates that the samples lack long-range order. The consistency between the SAXS patterns suggests that all stereoblock-containing samples display a similar morphology after processing and implies that the variations observed in the modulus are not related to gross morphological differences between the samples. The absence 10

of higher order peaks characteristic of lamellar morphologies indicates that crystallization in stereoblock-containing samples did not disrupt the melt-state morphology through crystalline breakout.<sup>11,43</sup>

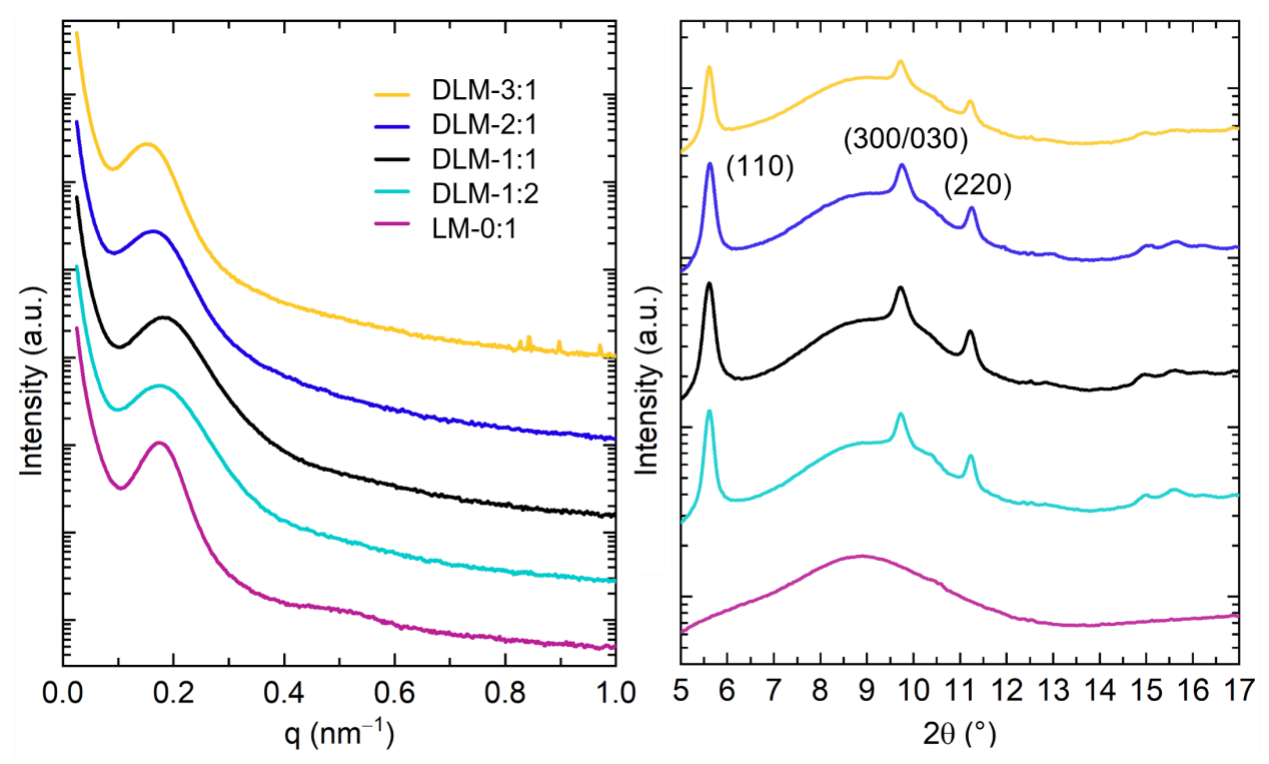


**Figure 3.** SAXS (left) and WAXS (right) patterns of stereoblock star terpolymers at room temperature with D:L block ratios of 3:1 (yellow), 2:1 (blue), 1:1 (black), 1:2 (aqua), and 0:1 (magenta). The patterns have been vertically shifted for clarity. The small peak at 10.5° in the WAXS patterns is due to background scattering from the aluminum pans in which samples were analyzed.

Variable temperature WAXS was also used to confirm the presence of SCs in the star terpolymers (**Figures S13-S17**). Unlike LM-0:1, which displays only a large amorphous halo at room temperature, the DLM stereoblocks all display clear diffraction peaks assigned to the (110), (300/030), and (220) planes of the SCs.<sup>19,53</sup> None of the DLM stereoblocks display peaks associated with PLLA or PDLA HCs at RT; the lack of observed HCs in the asymmetric samples

is contrary to previous reports for asymmetric PLLA and PDLA blends and linear ABCBA stereoblock polymers, which typically display WAXS diffraction peaks characteristic of both HCs and SCs.<sup>23,24,46,48,54,55</sup> However, exclusive stereocomplex crystallization has been observed in asymmetric linear stereo-diblocks with high molar masses.<sup>56</sup>

Stress relaxation is a measure of the time-dependent stress response to a fixed applied deformation. In TPEs, stress relaxation is typically associated with chain-pullout of the end blocks from the hard domains that releases trapped entanglements and allows for rearrangements of the polymer chains that relax stress with concomitant permanent deformation. 11,12,57,58 The impact of SCs and block ratio on the stress relaxation behavior in these APTPEs was investigated through uniaxial extensional rheology by applying a constant strain at varied temperatures and measuring the stress response over time. Samples were equilibrated for 10 min at the indicated temperature before application of a 25% step strain. The DLM stereoblocks relax less stress than the LM analogue at all temperatures investigated (Figure 4 top). For example, at 40 °C, the symmetric stereoblock DLM-1:1 relaxed only 35% of the applied stress while the LM-0:1 analogue relaxed 60% of the applied stress (Figure 4 top, blue curves) over 3 h. As observed in the WAXS and DSC data (Figure 3), the improved stress relaxation behavior can likely be attributed to the increased initial degree of crystallinity in the stereoblocks. This crystallinity-driven enhancement in stress relaxation behavior has been previously reported. 10 The enhanced stress relaxation behavior for the DLM stereoblocks showcases the improvements attained by the introduction of SCs into the hard domains in these APTPEs, given the common processing conditions employed for both samples.

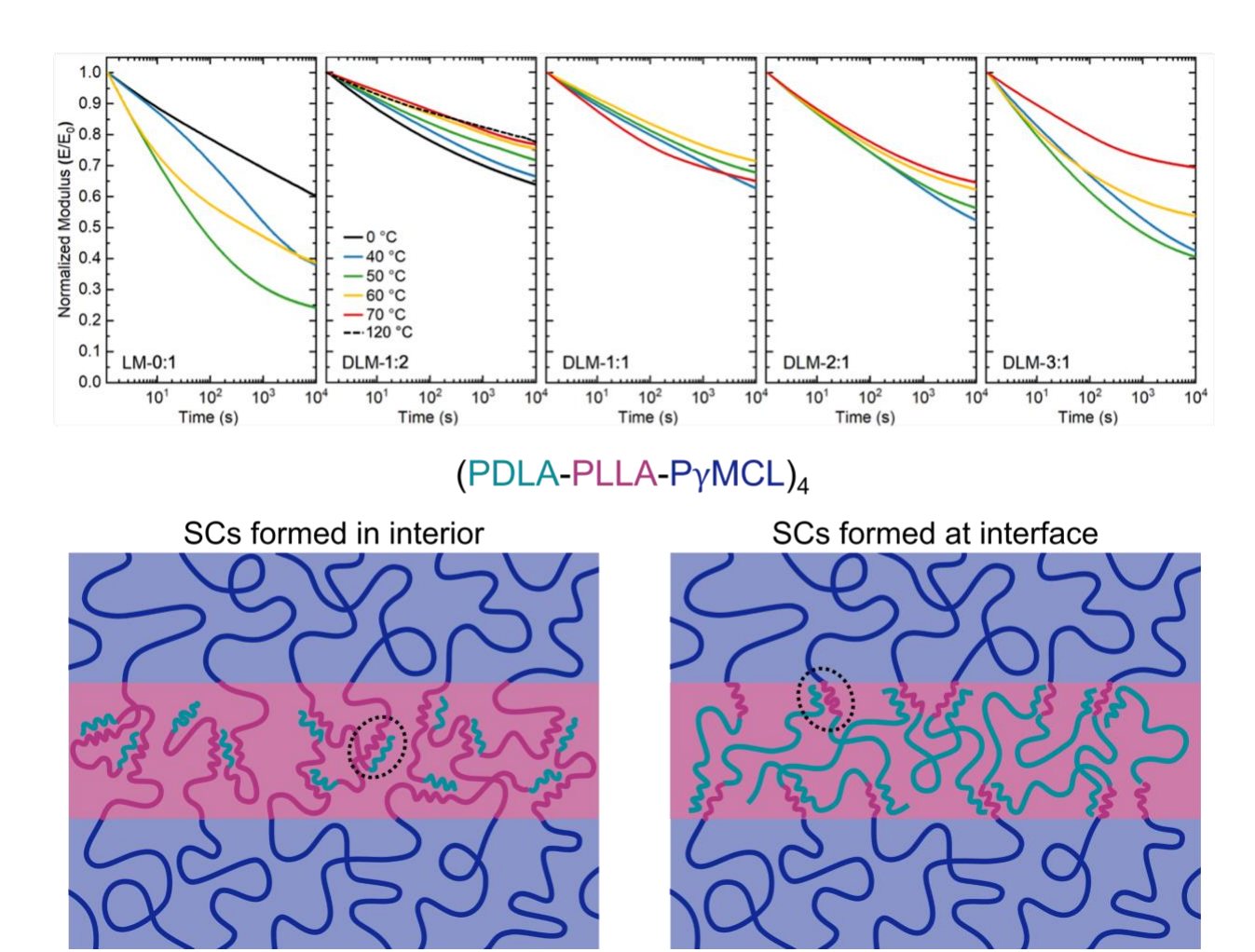


**Figure 4.** Stress relaxation of stereoblock star terpolymers with varied D:L block ratios at 0 °C (black), 40 °C (blue), 50 °C (green), 60 °C (yellow), and 70 °C (red) (top). Samples were held at a 25% strain for 3 h. The modulus values have been normalized to the initial modulus (t = 0) to allow for comparison between samples. Graphic representing conformational constraints to SC formation based on length of inner PLLA block (covalently bonded to rubbery midblock) (bottom).

The difference in the stress relaxation behavior of these systems may be due to conformational constraints associated with the sequencing and relative lengths of the PDLA and PLLA blocks. For systems where the inner PLLA block is shorter (i.e., DLM-2:1 and DLM-3:1), the stereocomplex is forced to form closer to the hard domain interface with the PγMCL matrix as they are constrained by the inner PLLA blocks pinned to the interface. In the cases where the inner PLLA block is longer or equivalent in length to the outer PDLA block (i.e., DLM-1:2 and DLM-1:2).

1:1) the SCs can form closer to the interior of the hard domains as the PDLA chain ends are not directly tethered to the rubbery PγMCL matrix (**Figure 4** bottom).<sup>59</sup> These constraints on the location for stereocomplex formation could impact their ability to mitigate chain pullout, with SCs buried deeper within the hard domains being more effective than those closer to the hard-soft interface.

Unexpectedly, the stress relaxation behavior of DLM-1:2, DLM-1:1, and DLM-2:1 at 50 °C, improves (i.e., relaxes less stress), while the remaining APTPEs show the expected trend of increased stress relaxation with increasing temperature (**Figure 4** top, green trace). However, when the temperature is increased to 60 °C, all APTPEs, including the LM analogue, exhibit superior stress relaxation behavior when compared to their performances at both 40 °C and 50 °C (**Figure 4** top, yellow trace). DSC studies of the samples after testing do not indicate a significant change in the enthalpy of fusion, suggesting that this improvement is not a result of increased crystallinity (**Figure S18**). The change in the shape of the stress relaxation curves between 40 and 60 °C suggests a change in the molecular mobility of the polymer chains upon passing through the  $T_g$  of PLA. This behavior persisted at even higher temperatures; for example, the DLM-1:2 stereoblocks only relaxed 25–30% of the applied stress at 120 °C, indicating impressive stress retention well above the  $T_g$  of PLLA (See **Figures S19 and S20**).

Representative stress-strain curves for the samples can be seen in **Figure S21** and average values with standard deviations for the Young's modulus (E), ultimate tensile strength ( $\sigma_B$ ), percent recovery, and elongation at break ( $\varepsilon_B$ ) are reported in **Table 1**. All of the samples display strain hardening behavior, resulting in high ultimate tensile strengths ( $\sigma_B = 30$ –45 MPa) and elongations at break ( $\varepsilon_B = 950$ –1250 %), indicating strong and highly extensible materials. The

ultimate tensile strength, percent recovery, and Young's modulus as a function of D-lactide content are shown in in **Figure 5**. The impressive ultimate tensile strengths of the samples are competitive with commercial materials and suitable for high-performance applications. While the ultimate tensile strengths of these APTPEs remain fairly consistent, there is variation in the Young's moduli and recovery behavior for the samples as a function of the D-lactide content.

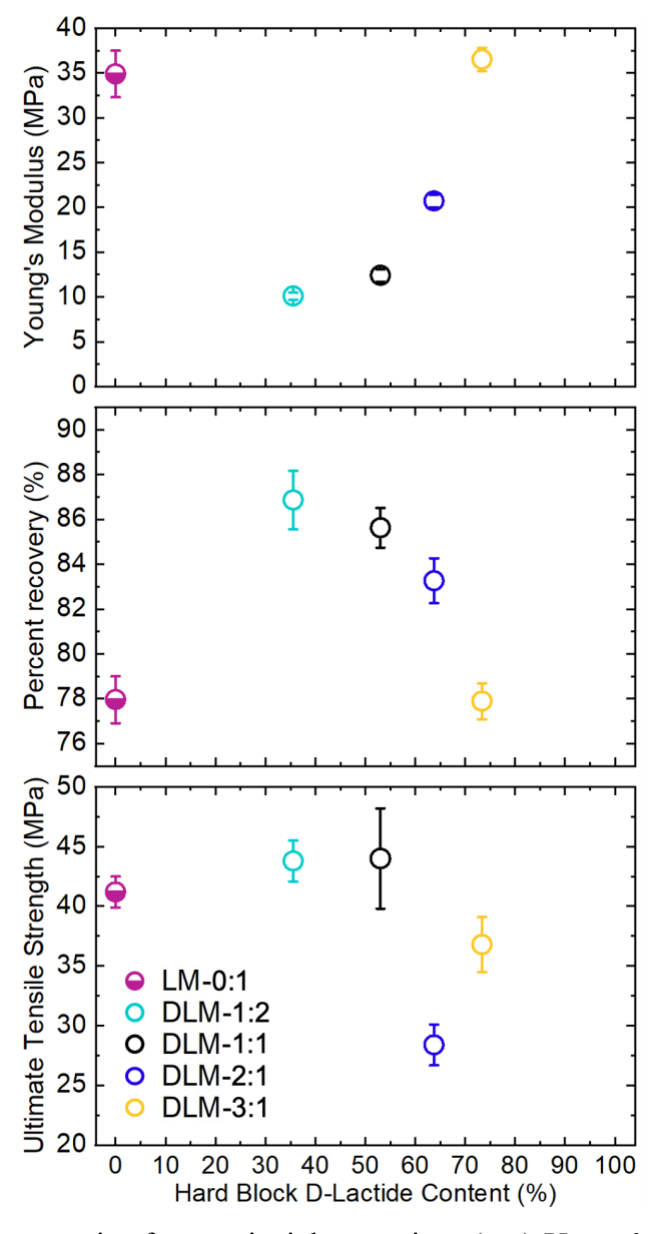


**Figure 5.** Mechanical properties from uniaxial extension: (top) Young's modulus (E), (middle) percent recovery, and (bottom) ultimate tensile strength ( $\sigma_B$ ), of stereoblock star terpolymers with

D:L block ratios of 0:1 (magenta, half filled), 1:2 (aqua, open), 1:1 (black, open), 2:1 (blue, open), and 3:1 (yellow, open). Samples were extended at 50 mm min<sup>-1</sup> with percent recovery calculated from residual strain after 10 cycles of a 300% strain.

Similar to the trend observed in the initial plateau modulus by DMTA, the Young's modulus and percent recovery values vary with the D-lactide content of the material. Samples containing higher D-lactide content showed higher Young's modulus values with more plasticlike behavior (i.e., lower percent recovery) (**Figure 5**) which may be a result of confinement effects on stereocomplex formation induced by the arm architecture. The observed variation in both the Young's modulus and precent recovery values for the DLM stereoblocks indicate tunable stiffnesses while maintaining high tensile strengths and strains at break. Typically, to achieve such differences in the Young's moduli, changes to the overall hard block volume fraction or polymer architecture are required which can negatively impact elastomeric behavior or lead to undesirable microstructured morphologies and processing difficulties. In these materials, we have demonstrated that simply changing the D:L composition of the hard blocks can produce APTPEs with tunable mechanical properties for an array of applications. This enhanced understanding of the impact of SCs within TPEs will enable the development of new materials with differing hard block loadings and varying molar masses to further improve material design and our understanding of the impact of architecture on TPE performance.

## Acknowledgements

We would like to acknowledge Caitlin Sample, Claire Dingwell, Daniel Krajovic and Marianne Meyersohn for many helpful discussions. Ortec, Inc. generously provided lactide. SAXS experiments were performed at the DuPont-Northwestern-Dow Collaborative Access Team (DND-CAT) located at Sector 5 of the Advanced Photon Source (APS). DND-CAT is supported

by the Northwestern University, E.I. DuPont de Nemours & Co., and Dow Chemical Company. This research used resources of the Advanced Photon Source, a U.S. Department of Energy (DOE) Office of Science user facility operated for the U.S. DOE Office of Science by the Argonne National Laboratory under contract no. DE-AC02-06CH11357. Graphics creation was assisted by John Beumer with the NSF Center for Sustainable Polymers. We also acknowledge the NSF Center for Sustainable Polymers (CHE-1901635), as well as the 3M Science and Technology Fellowship.

#### **Associated Content**

## **Supporting Information**

Materials and methods; detailed synthetic procedures, processing methods, and characterization details: <sup>1</sup>H NMR spectra, SAXS spectra, WAXS spectra, DMTA data, DSC data, SEC data, tensile data, and stress relaxation data (**Tables S1–S4** and **Figures S1–S21**).

#### References

- (1) Holden, G.; Kricheldorf, H. R.; Quirk, R. P. *Thermoplastic Elastomers*; Holden, G., Kricheldorf, H. R., Quirk, R. P., Eds.; Hanser Gardner Publications, Inc.: Cincinnati, 2004.
- (2) Matsen, M. W.; Thompson, R. B. Equilibrium Behavior of Symmetric ABA Triblock Copolymer Melts. *J. Chem. Phys.* **1999**, *111* (15), 7139–7146.
- (3) Drobny, J. G. Handbook of Thermoplastic Elastomers; Elsevier, 2014.
- (4) Chamas, A.; Moon, H.; Zheng, J.; Qiu, Y.; Tabassum, T.; Jang, J. H.; Abu-Omar, M.; Scott, S. L.; Suh, S. Degradation Rates of Plastics in the Environment. *ACS Sustain. Chem. Eng.* **2020**, *8* (9), 3494–3511.
- (5) Wanamaker, C. L.; O'Leary, L. E.; Lynd, N. A.; Hillmyer, M. A.; Tolman, W. B. Renewable-Resource Thermoplastic Elastomers Based on Polylactide and Polymenthide. *Biomacromolecules* **2007**, *8* (11), 3634–3640.
- (6) Martello, M. T.; Hillmyer, M. A. Polylactide-Poly(6-Methyl-ε-Caprolactone)-Polylactide Thermoplastic Elastomers. *Macromolecules* **2011**, *44* (21), 8537–8545.
- (7) Martello, M. T.; Schneiderman, D. K.; Hillmyer, M. A. Synthesis and Melt Processing of Sustainable Poly(ε-Decalactone)-Block-Poly(Lactide) Multiblock Thermoplastic Elastomers. *ACS Sustain. Chem. Eng.* **2014**, *2* (11), 2519–2526.

- (8) Schneiderman, D. K.; Hillmyer, M. A. 50th Anniversary Perspective: There Is a Great Future in Sustainable Polymers. *Macromolecules* **2017**, *50* (10), 3733–3749.
- (9) Xiong, M.; Schneiderman, D. K.; Bates, F. S.; Hillmyer, M. A.; Zhang, K. Scalable Production of Mechanically Tunable Block Polymers from Sugar. *Proc. Natl. Acad. Sci.* **2014**, *111* (23), 8357–8362.
- (10) Watts, A.; Kurokawa, N.; Hillmyer, M. A. Strong, Resilient, and Sustainable Aliphatic Polyester Thermoplastic Elastomers. *Biomacromolecules* **2017**, *18* (6), 1845–1854.
- (11) Watts, A.; Hillmyer, M. A. Aliphatic Polyester Thermoplastic Elastomers Containing Hydrogen-Bonding Ureidopyrimidinone Endgroups. *Biomacromolecules* **2019**, *20* (7), 2598–2609.
- (12) Liffland, S.; Hillmyer, M. A. Enhanced Mechanical Properties of Aliphatic Polyester Thermoplastic Elastomers through Star Block Architectures. *Macromolecules* **2021**, *54* (20), 9327–9340.
- (13) Blankenship, J. R.; Levi, A. E.; Goldfeld, D. J.; Self, J. L.; Alizadeh, N.; Chen, D.; Fredrickson, G. H.; Bates, C. M. Asymmetric Miktoarm Star Polymers as Polyester Thermoplastic Elastomers. *Macromolecules* **2022**, *55* (12), 4929–4936.
- (14) Auras, R. A.; Harte, B.; Selke, S.; Hernandez, R. Mechanical, Physical, and Barrier Properties of Poly(Lactide) Films. *J. Plast. Film Sheeting* **2003**, *19* (2), 123–135.
- (15) *Polymer Handbook*, 4th ed.; Brandrup, J., Immergut, E. H., Grulke, E. A., Eds.; Wiley: New York, 1999.
- (16) Liao, R.; Yang, B.; Yu, W.; Zhou, C. Isothermal Cold Crystallization Kinetics of Polylactide/Nucleating Agents. *J. Appl. Polym. Sci.* **2007**, *104* (1), 310–317.
- (17) Ahmed, J.; Arfat, Y. A. Polylactides: Properties and Applications. *Kirk-Othmer Encycl. Chem. Technol.* **2016**, 1–18.
- (18) Dechy-Cabaret, O.; Martin-Vaca, B.; Bourissou, D. Controlled Ring-Opening Polymerization of Lactide and Glycolide. *Chem. Rev.* **2004**, *104* (12), 6147–6176.
- (19) Ikada, Y.; Jamshidi, K.; Tsuji, H.; Hyon, S. H. Stereocomplex Formation between Enantiomeric Poly(Lactides). *Macromolecules* **1987**, *20* (4), 904–906.
- (20) Tsuji, H. Poly(Lactide) Stereocomplexes: Formation, Structure, Properties, Degradation, and Applications. *Macromol. Biosci.* **2005**, *5* (7), 569–597.
- (21) Tsuji, H. In Vitro Hydrolysis of Blends from Enantiomeric Poly(Lactide)s Part 1. Well-Stereo-Complexed Blend and Non-Blended Films. *Polymer* **2000**, *41* (10), 3621–3630.
- (22) Tsuji, H.; Ikada, Y. Stereocomplex Formation between Enantiomeric Poly(Lactic Acid)s. XI. Mechanical Properties and Morphology of Solution-Cast Films. *Polymer* **1999**, *40* (24), 6699–6708.
- (23) Schmidt, S. C.; Hillmyer, M. A. Polylactide Stereocomplex Crystallites as Nucleating Agents for Isotactic Polylactide. *J Polym Sci B Polym Phys* **2001**, *39*, 300–313.
- (24) Anderson, K. S.; Hillmyer, M. A. Melt Preparation and Nucleation Efficiency of Polylactide Stereocomplex Crystallites. *Polymer* **2006**, *47* (6), 2030–2035.
- (25) Tsuji, H.; Fukui, I. Enhanced Thermal Stability of Poly(Lactide)s in the Melt by Enantiomeric Polymer Blending. *Polymer* **2003**, *44* (10), 2891–2896.
- (26) Brochu, S.; Prud'homme, R. E.; Barakat, I.; Jerome, R.; Jérôme, R. Stereocomplexation and Morphology of Polylactides. *Macromolecules* **1995**, *28* (15), 5230–5239.

- (27) Brizzolara, D.; Cantow, H.-J.; and, K. D.; Keller, E.; Domb, A. J. Mechanism of the Stereocomplex Formation between Enantiomeric Poly(Lactide)s. *Macromolecules* **1996**, *29* (1), 191–197.
- (28) Spinu, M.; Jackson, C.; Keating, M. Y.; Gardner, K. H. Material Design in Poly(Lactic Acid) Systems: Block Copolymers, Star Homo- and Copolymers, and Stereocomplexes. *J. Macromol. Sci. Part A* **1996**, *33* (10), 1497–1530.
- (29) Sarasua, J.-R.; Prud'homme, R. E.; Wisniewski, M.; Le Borgne, A.; Spassky, N. Crystallization and Melting Behavior of Polylactides. *Macromolecules* **1998**, *31* (12), 3895–3905.
- (30) Li, L.; Zhong, Z.; de Jeu, W. H.; Dijkstra, P. J.; Feijen, J. Crystal Structure and Morphology of Poly(l-Lactide-b-d-Lactide) Diblock Copolymers. *Macromolecules* **2004**, *37* (23), 8641–8646.
- (31) Isono, T.; Kondo, Y.; Ozawa, S.; Chen, Y.; Sakai, R.; Sato, S.; Tajima, K.; Kakuchi, T.; Satoh, T. Stereoblock-like Brush Copolymers Consisting of Poly(l-Lactide) and Poly(d-Lactide) Side Chains along Poly(Norbornene) Backbone: Synthesis, Stereocomplex Formation, and Structure–Property Relationship. *Macromolecules* **2014**, *47* (20), 7118–7128.
- (32) Fukushima, K.; Kimura, Y. An Efficient Solid-State Polycondensation Method for Synthesizing Stereocomplexed Poly(Lactic Acid)s with High Molecular Weight. *J. Polym. Sci. Part Polym. Chem.* **2008**, *46* (11), 3714–3722.
- (33) Tsuji, H.; Wada, T.; Sakamoto, Y.; Sugiura, Y. Stereocomplex Crystallization and Spherulite Growth Behavior of Poly(l-Lactide)-b-Poly(d-Lactide) Stereodiblock Copolymers. *Polymer* **2010**, *51* (21), 4937–4947.
- (34) Rahaman, Md. H.; Tsuji, H. Synthesis and Characterization of Stereo Multiblock Poly(Lactic Acid)s with Different Block Lengths by Melt Polycondensation of Poly(L-Lactic Acid)/Poly(D-Lactic Acid) Blends. *Macromol. React. Eng.* **2012**, *6* (11), 446–457.
- (35) Han, L.; Shan, G.; Bao, Y.; Pan, P. Exclusive Stereocomplex Crystallization of Linear and Multiarm Star-Shaped High-Molecular-Weight Stereo Diblock Poly(Lactic Acid)s. *J. Phys. Chem. B* **2015**, *119* (44), 14270–14279.
- (36) Isono, T.; Kondo, Y.; Otsuka, I.; Nishiyama, Y.; Borsali, R.; Kakuchi, T.; Satoh, T. Synthesis and Stereocomplex Formation of Star-Shaped Stereoblock Polylactides Consisting of Poly(L-Lactide) and Poly(D-Lactide) Arms. *Macromolecules* **2013**, *46* (21), 8509–8518.
- (37) Tsuji, H.; Matsumura, N.; Arakawa, Y. Stereocomplex Crystallization and Homocrystallization of Star-Shaped Four-Armed Stereo Diblock Poly(Lactide)s with Different L-Lactyl Unit Contents: Isothermal Crystallization from the Melt. *J. Phys. Chem. B* **2016**, *120* (6), 1183–1193.
- (38) Tsuji, H.; Matsumura, N.; Arakawa, Y. Stereocomplex Crystallization and Homo-Crystallization of Star-Shaped Four-Armed Stereo Diblock Poly(Lactide)s during Precipitation and Non-Isothermal Crystallization. *Polym. J.* **2016**, *48* (11), 1087–1093.
- (39) Hirata, M.; Masutani, K.; Kimura, Y. Synthesis of ABCBA Penta Stereoblock Polylactide Copolymers by Two-Step Ring-Opening Polymerization of l- and d-Lactides with Poly(3-Methyl-1,5-Pentylene Succinate) as Macroinitiator (C): Development of Flexible Stereocomplexed Polylactide Materials. *Biomacromolecules* **2013**, *14* (7), 2154–2161.
- (40) Lee, C. W.; Na, C.; Kimura, Y.; Masutani, K. ABCBA Pentablock Copolymers Consisting of Poly(l-Lactide) (PLLA: A), Poly(d-Lactide) (PDLA: B), and Poly(Butylene Succinate)

- (PBS: C): Effects of Semicrystalline PBS Segments on the Stereo-Crystallinity and Properties. *Macromol. Mater. Eng.* **2016**, *301* (9), 1121–1131.
- (41) Nishiwaki, Y.; Masutani, K.; Kimura, Y.; Lee, C.-W. Synthesis and Mechanochemical Properties of Biobased ABCBA-Type Pentablock Copolymers Comprising Poly-d-Lactide (A), Poly-l-Lactide (B) and Poly(1,2-Propylene Succinate) (C). *J. Polym. Sci.* **2022**, *60* (14), 2043–2054.
- (42) Slomkowski, S.; Penczek, S.; Duda, A. Polylactides-an Overview. *Polym. Adv. Technol.* **2014**, *25* (5), 436–447.
- (43) Nandan, B.; Hsu, J. Y.; Chen, H. L. Crystallization Behavior of Crystalline-Amorphous Diblock Copolymers Consisting of a Rubbery Amorphous Block. *Polym. Rev.* **2006**, *46* (2), 143–172.
- (44) Loo, Y. L.; Register, R. A.; Ryan, A. J. Modes of Crystallization in Block Copolymer Microdomains: Breakout, Templated, and Confined. *Macromolecules* **2002**, *35* (6), 2365–2374.
- (45) Honeker, C. C.; Thomas, E. L. Impact of Morphological Orientation in Determining Mechanical Properties in Triblock Copolymer Systems. *Chem. Mater.* **1996**, *8* (8), 1702–1714.
- (46) Wanamaker, C. L.; Tolman, W. B.; Hillmyer, M. A. Poly(D-Lactide)—Poly(Menthide)—Poly(D-Lactide) Triblock Copolymers as Crystal Nucleating Agents for Poly(L-Lactide). *Macromol. Symp.* **2009**, 283–284 (1), 130–138.
- (47) Tsuji, H.; Yamashita, Y. Highly Accelerated Stereocomplex Crystallization by Blending Star-Shaped 4-Armed Stereo Diblock Poly(Lactide)s with Poly(d-Lactide) and Poly(l-Lactide) Cores. *Polymer* **2014**, *55* (25), 6444–6450.
- (48) Tsuji, H.; Takai, H.; Saha, S. K. Isothermal and Non-Isothermal Crystallization Behavior of Poly(l-Lactic Acid): Effects of Stereocomplex as Nucleating Agent. *Polymer* **2006**, *47* (11), 3826–3837.
- (49) Zhang, X.; Meng, L.; Li, G.; Liang, N.; Zhang, J.; Zhu, Z.; Wang, R. Effect of Nucleating Agents on the Crystallization Behavior and Heat Resistance of Poly(l-Lactide). *J. Appl. Polym. Sci.* **2016**, *133* (8).
- (50) Li, W.; Wu, X.; Chen, X.; Fan, Z. The Origin of Memory Effect in Stereocomplex Poly (Lactic Acid) Crystallization from Melt State. *Eur. Polym. J.* **2017**, *89*, 241–248.
- (51) Huang, Y. F.; Zhang, Z. C.; Li, Y.; Xu, J. Z.; Xu, L.; Yan, Z.; Zhong, G. J.; Li, Z. M. The Role of Melt Memory and Template Effect in Complete Stereocomplex Crystallization and Phase Morphology of Polylactides. *Cryst. Growth Des.* **2018**, *18* (3), 1613–1621.
- (52) Bates, F. S.; Fredrickson, G. H. Block Copolymer Thermodynamics: Theory and Experiment. *Annu. Rev. Phys. Chem.* **1990**, *41* (1), 525–557.
- (53) Okihara, T.; Tsuji, M.; Kawaguchi, A.; Katayama, K. I.; Tsuji, H.; Hyon, S. H.; Ikada, Y. Crystal Structure of Stereocomplex of Poly(L-Lactide) and Poly(D-Lactide). *J. Macromol. Sci. Part B* **1991**, *30* (1–2), 119–140.
- (54) Tsuji, H.; Ikada, Y. Stereocomplex Formation between Enantiomeric Poly(Lactic Acid)s. 9. Stereocomplexation from the Melt. *Macromolecules* **1993**, *26* (25), 6918–6926.
- (55) Tsuji, H.; Ikada, Y. Stereocomplex Formation between Enantiomeric Poly(Lactic Acid)s. 6. Binary Blends from Copolymers. *Macromolecules* **1992**, *25* (21), 5719–5723.

- (56) Hirata, M.; Kobayashi, K.; Kimura, Y. Synthesis and Properties of High-Molecular-Weight Stereo Di-Block Polylactides with Nonequivalent D/L Ratios. *J. Polym. Sci. Part Polym. Chem.* **2010**, *48* (4), 794–801.
- (57) Burns, A. B.; Register, R. A. Mechanical Properties of Star Block Polymer Thermoplastic Elastomers with Glassy and Crystalline End Blocks. *Macromolecules* **2016**, *49* (24), 9521–9530.
- (58) Hotta, A.; Clarke, S. M.; Terentjev, E. M. Stress Relaxation in Transient Networks of Symmetric Triblock Styrene-Isoprene-Styrene Copolymer. *Macromolecules* **2002**, *35* (1), 271–277.
- (59) Milner, S. T.; McLeish, T. C. B. Arm-Length Dependence of Stress Relaxation in Star Polymer Melts. *Macromolecules* **1998**, *31* (21), 7479–7482.